Available online at www.sciencedirect.com
SCIENCE DIRECT®
ELSEVIER
Antiviral Research xxx (2006) xxx–xxx
Antiviral Research
www.elsevier.com/locate/antiviral

Cooperative contribution of gag substitutions to nelfinavir-dependent enhancement of precursor cleavage and replication of human immunodeficiency virus type-1

Saori Matsuoka-Aizawa [a,b], Hiroyuki Gatanaga [a,*], Hironori Sato [c], Kazuhiko Koike [b], Satoshi Kimura [a], Shinichi Oka [a]

[a] *AIDS Clinical Center, International Medical Center of Japan, 1-21-1, Toyama, Shinjuku-ku, Tokyo 162-8655, Japan*
[b] *Graduate School of Medicine, University of Tokyo, Japan*
[c] *Division of Molecular Genetics, National Institute of Infectious Diseases, Tokyo, Japan*

Received 9 June 2005; accepted 11 January 2006

Abstract

We previously described a clinical human immunodeficiency virus type-1 (HIV-1) isolate, CL-4, which showed nelfinavir (NFV)-dependent enhancement of replication (Matsuoka-Aizawa, S., Sato, H., Hachiya, A., Tsuchiya, K., Takebe, Y., Gatanaga, H., Kimura, S., Oka, S, 2003. Isolation and molecular characterization of a nelfinavir (NFV)-resistant human immunodeficiency virus type 1 that exhibits NFV-dependent enhancement of replication. J. Virol. 77, 318–327.). To identify the responsible region(s) of HIV-1 proteins for such replication enhancement, we constructed a panel of recombinant HIV-1 clones harboring portions of the Gag and protease of CL-4 and analyzed their replication capabilities and Gag processing patterns. Our data suggested that the substitutions in the matrix and N-terminal half of capsid of CL-4 were indispensable for the NFV-dependent enhancement of replication and that NFV facilitated the cleavage between the matrix and capsid of the Gag precursor harboring these substitutions. The substitutions in C-terminal half of capsid rather decreased the cleavability of Gag precursor and NFV counteracted such negative impact. Efficient replication enhancement with NFV can be observed only in the presence of the substitutions in entire Gag and protease of CL-4.

Keywords: Human immunodeficiency virus type 1; Nelfinavir-resistant; Gag mutation

1. Introduction

Under the selective pressure of antiretroviral agents, the human immunodeficiency virus type-1 (HIV-1) evolves and acquires drug-resistance-associated mutations. The major protease inhibitor (PI)-resistance-associated mutations are located in the active sites of HIV-1 protease and impair its enzymatic functions (Bleiber et al., 2001; Croteau et al., 1997; Martinez-Picado et al., 1999). In order to compensate such impaired enzymatic function, PI-resistant HIV-1 further acquires mutations not only in protease but also in one of its substrate, Gag, resulting in full recovery of replication ability (Doyon et al., 1996; Gatanaga et al., 2002; Tamiya et al., 2004; Zhang et al., 1997). We previously described a unique clinical HIV-1 isolate, CL-4, which replicated more efficiently in the presence of sub-inhibitory concentrations of nelfinavir (NFV) (0.001–0.1 μM) (Matsuoka-Aizawa et al., 2003). CL-4 had a total of 56 amino acid substitutions in *gag-pro* genes compared with NL4-3; 22 substitutions had emerged in the matrix, SP1, and protease during administration of NFV-containing therapy, and 34 other substitutions had already existed before the introduction of the therapy (Matsuoka-Aizawa et al., 2003). In that study, we constructed three HIV-1 clones including, p17PRmt, PRmt, and p24PRmt, and found that only p17PRmt, which possessed the entire Gag and protease segment of CL-4, showed NFV-dependent enhancement of replication. Therefore, we concluded that the substitutions in matrix are indispensable for replication enhancement (Matsuoka-Aizawa et al., 2003). However, it is still unknown whether the substitutions in matrix alone are sufficient or whether other Gag substitutions are necessary for the replication enhancement with NFV. In this study we constructed four more recombinant HIV-1 clones and characterized their replica-

* Corresponding author. Tel.: +81 3 5273 5193; fax: +81 3 5273 5193.
E-mail address: higatana@imcj.acc.go.jp (H. Gatanaga).

0166-3542/$ – see front matter © 2006 Elsevier B.V. All rights reserved.
doi:10.1016/j.antiviral.2006.01.004

tion kinetics and Gag processing in the absence and presence of NFV.

2. Materials and methods

2.1. Cells and antiretroviral agents

HeLa cells were maintained in Dulbecco's minimal essential medium (DMEM) supplemented with 10% fetal calf serum (FCS). Transformed T cell lines, MT-2, PM-1, and H9 cells were maintained in RPMI-1640 with 10% FCS. NFV was kindly provided by the Japan Tobacco Co. (Tokyo, Japan).

2.2. Plasmid construction and preparation of gag-pro recombinant HIV-1 clones

Clinical HIV-1 isolates CL-1, CL-2, CL-3, and CL-4 were sequentially obtained from the same patient before and during NFV-containing treatment (Matsuoka-Aizawa et al., 2003). Direct sequences of these four clinical isolates and sub-cloning

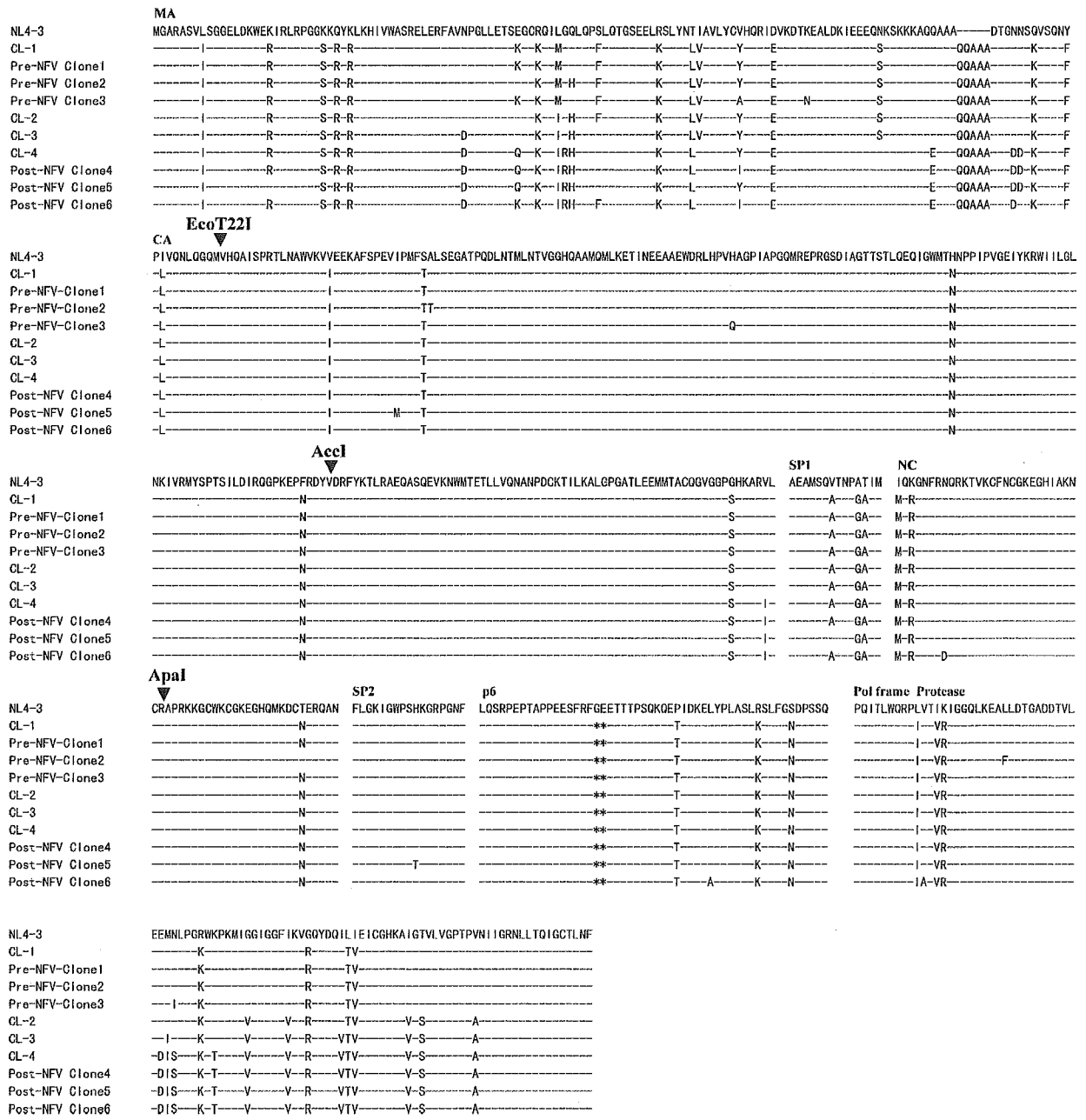

Fig. 1. Direct and sub-clonal sequences of clinical HIV-1 isolates. Direct and sub-clonal amino acid sequences of whole Gag and protease of HIV-1 isolates are shown. Pre-NFV Clone 1–3 and Post-NFV Clone 4–6 were derived from CL-1 and CL-4, respectively. The amino acid sequence of HIV-1_{NL4-3} is shown at the top as reference. The identical amino acids with those of HIV-1_{NL4-3} are indicated with dashes and the star shows deletion compared with HIV-1_{NL4-3} sequence. The restriction sites used in the construction of recombinant HIV-1 plasmids are also shown. MA, matrix; CA, Capsid; NC, nucleocapsid; and PR, protease.

sequences of CL-1 and CL-4 indicated that 11 and 10 amino acid substitutions accumulated in Gag and protease during PI-containing treatment, respectively (Fig. 1). Post-NFV Clone 4 (Fig. 1) was used in the construction of CL-4-derived recombinant HIV-1 plasmid. The pNL4-3-based plasmids of PRmt (HIV-1 carrying only the substitutions in protease of CL-4), p24PRmt (carrying the substitutions in capsid and protease of CL-4), and p17PRmt (carrying the substitutions in whole Gag and protease of CL-4) were constructed as previously described (Matsuoka-Aizawa et al., 2003) (Fig. 2), and the plasmids of MAmt (carrying only the substitutions in the matrix of CL-4) and MA + PRmt (carrying the substitutions in the matrix and protease of CL-4) were constructed by using the same restriction enzyme sites (Figs. 1 and 2). The plasmids of NCAmt (carrying the substitutions in matrix, N-terminal half of capsid, and protease of CL-4) and CCAmt (carrying the substitutions in matrix, C-terminal half of capsid, and protease of CL-4) were constructed by using AccI site. Originally, pNL4-3 has two AccI site between *gag* and protease region, one in the matrix, and the other in the capsid. However, since the one in the matrix was extinct due to natural substitution in CL-4, the other in the capsid was unique in *gag* and protease region.

HeLa cells (5×10^5 cells) were grown in DMEM with 10% FCS for 24 h and transfected with 3 μg of pNL4-3 and *gag*-protease recombinant HIV-1 plasmid DNAs by using FuGINE 6 transfection reagent (Roche Diagnosis, Basel, Switzerland). The cells were incubated for 24 h, washed once with PBS, and cultured in 5 ml of culture medium. The culture supernatant containing virus was collected at 48 h after transfection, filtered, analyzed for RT activity (10432–17162 cpm/μM), and kept at −80 °C until use. The virus titer used for infection and Western blot analysis was adjusted with RT activity.

2.3. HIV-1 replication kinetics

The methods used to infect cells were described previously (Matsuoka-Aizawa et al., 2003). Briefly, MT-2, PM-1, and H9 cells (2×10^4) were infected with 200 μl of cell-free supernatant containing HIV-1 (2×10^5 ^{32}P cpm of RT activity) in the absence or presence of NFV (0.1 and 1 μM) for 16 h, washed once, and cultured in 200 μl of culture medium with the same concentration of NFV. A half volume of culture medium was changed every 2 or 3 days, and the supernatant was kept at −80 °C for measurement of RT activity. Each experiment was carried out in duplicate and repeated three times.

2.4. Competitive HIV-1 replication assay

H9 cells (2×10^5 cells) were incubated with two HIV-1 clones (each of 100 $TCID_{50}$) simultaneously for 16 h, washed with PBS twice, and cultured in the absence or presence of 0.1 μM NFV for 7 days. These infection periods were defined as a single passage. At the end of each passage, H9 cells were harvested and the culture supernatants were used to infect fresh

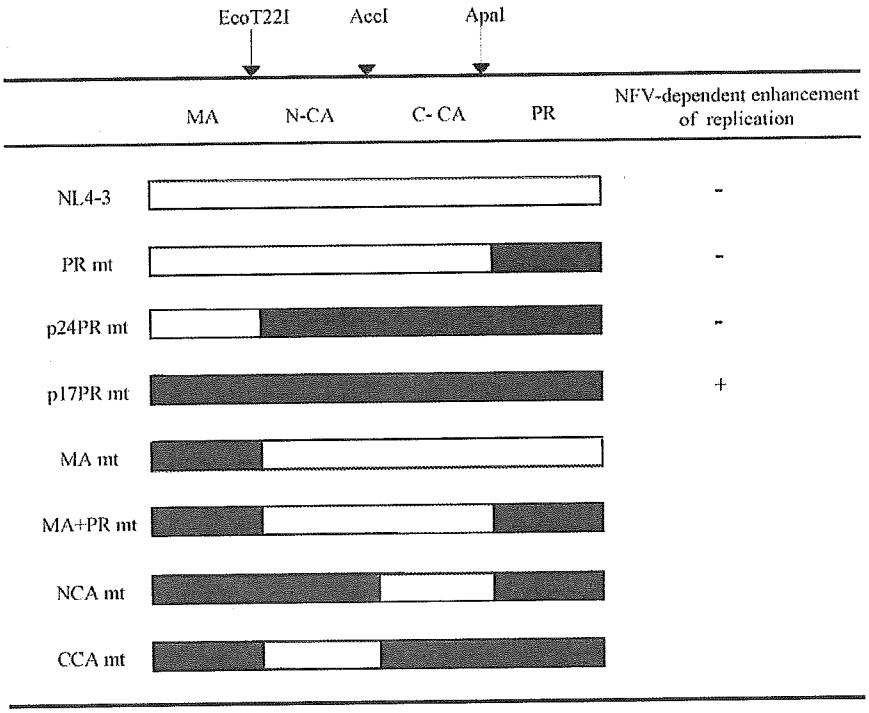

Fig. 2. Previously and newly constructed recombinant HIV-1s. The recombinant molecular clones were constructed based on pNL4-3 as a genetic backbone. The Gag-PR region of HIV-1 was segmented into four areas, MA (BssHII-EcoT22I fragment), N-terminal half of CA (NCA) (EcoT22I-AccI fragment), C-terminal half of CA (CCA) (AccI-ApaI fragment), and PR (ApaI-BalI fragment). Originally, pNL4-3 has two AccI sites between the gag and PR region, in MA and CA. However, because the one in MA was extinct in CL-4 due to natural substitution, the other AccI site in CA was unique for gag-PR gene of CL-4. Open boxes indicate the NL4-3-originated fragments, and closed boxes indicate fragments that were derived from CL-4 variants. The NFV-dependent replication enhancement of previously analyzed clones was also shown and indicated as (+). MA, matrix; CA, capsid; and PR, protease.

uninfected H9 cells. The cells harvested at each passage were subjected to PCR for amplification of HIV-1 *gag* region and direct DNA sequencing was performed. The viral populational changes were determined by relative peak height on sequence electrophoregram (Kosalaraksa et al., 1999).

2.5. HIV-1 susceptibility to NFV

MT-2 cells were infected with 500 $TCID_{50}$ of each virus in the absence and the presence of 0.001, 0.00316, 0.01, 0.0316, 0.1, 0.316, 1, and 3.16 μM of NFV, and cultured in triplicate for 7 days. At the end of culture, the amounts of p24 in the supernatants were measured and 50% inhibitory concentrations (IC_{50}) of NFV were determined by referring to the dose–response curve.

2.6. Western blot analysis of HIV-1 virions

HeLa cells were transfected with pNL4-3 and *gag*-protease recombinant HIV-1 plasmid DNA in the absence and presence of 0.1 μM NFV. The culture supernatant was harvested at 48 h after transfection, centrifuged at 37,000 × *g* for 90 min to pellet virus particles. The virion pellet (6×10^5 cpm of RT activity) was applied to an SDS gradient gel electrophoresis and transferred to a nitrocellulose membrane. The membrane was incubated with anti-HIV-1 p24 antisera (Advanced Biotechnology, Columbia, USA) and HIV-1-infected patients' serum, respectively, and hybridized with anti-protein A antibody conjugated with horseradish peroxidase (Amersham Pharmacia Biotech, Uppsala, Sweden). The immune complex was visualized with an ECL Plus system (Amersham Pharmacia Biotech) according to the manufactures' description.

The percent signal density of Gag products was analyzed on a Windows computer by using the ImageJ Program (developed at the U.S. National Institutes of Health ⟨http://www.rsb.info.nih.gov/ij/⟩) and the percent density of p24 was determined by the following formula: percent density of p24 = 100 × (the density of p24 signal)/(the cumulated density of all *Gag* signals) (Tamiya et al., 2004).

3. Results

3.1. Whole capsid substitutions necessary for NFV-enhanced replication

MAmt, carrying only the substitutions in the matrix (Fig. 2), grew well in the absence of NFV (Fig. 3). In the presence of NFV, however, it did not grow at all, indicating that matrix substitutions were not sufficient to confer NFV resistance. MA + PRmt, carrying substitutions in the matrix and protease (Fig. 2), replicated as efficiently as PRmt (carrying only the substitutions in protease), both in the absence and presence of 0.1 μM NFV, though its replication was not enhanced with NFV, indicating that the substitutions in matrix and protease were not sufficient for NFV-dependent enhancement of replication. As reported in our previous study (Matsuoka-Aizawa et al., 2003), p17PRmt replicated more efficiently in the presence of 0.1 μM NFV than in the absence of NFV. Therefore, some of the substitutions in the capsid should be responsible for such unique phenotype of CL-4 strain. The HIV-1 capsid contains two domains, a C-terminal oligomerization domain and N-terminal core domain, which function differently in viral assembly (Turner and Summers, 1999). Therefore, we divided the EcoT22I—ApaI segment of CL-4 into two segments at ACC I site, named them the N-terminal half of the capsid (NCA) and the C-terminal half of the capsid (CCA), and constructed two recombinant HIV-1 clones, NCAmt and CCAmt, which possessed all the substitutions in the matrix and protease of CL-4, and the substitutions in NCA and CCA, respectively (Fig. 2). NCAmt and CCAmt grew efficiently both in the absence and presence of 0.1 μM NFV, and only NCAmt showed weak replication enhancement with 0.1 μM NFV in PM-1 and MT-2 cells though it was not so efficient as that of p17PRmt, suggesting that the substitutions in CCA, contributed to the efficient replication enhancement of p17PRmt (Fig. 3). CCAmt did not show the p17PRmt's phenotype, indicating that the substitutions in NCA were indispensable for replication enhancement. As we reported previously (Matsuoka-Aizawa et al., 2003), p24PRmt lacking the substitutions in matrix did not show replication enhancement by NFV. Taken together, the substitutions in the whole matrix, capsid, SP1, and the N-terminal end of nucleocapsid of CL-4 were indispensable for efficient replication enhancement of p17PRmt.

To define further the role of substitutions in the matrix, NCA, and CCA, viral replication efficiency was compared among the HIV-1 clones described above in the absence and presence of NFV using competitive HIV-1 replication assay (Kosalaraksa et al., 1999). MA + PRmt outgrew PRmt both in the absence and presence of 0.1 μM NFV (Fig. 4a), and MAmt was outgrown by NL4-3 in the absence of NFV (Fig. 4b), suggesting that the substitutions in the matrix of CL-4 reduced the replication of HIV-1 harboring wild-type protease, but compensated the replication of HIV-1 harboring NFV-resistant protease of CL-4. NCAmt outgrew MA + PRmt both in the absence and presence of 0.1 μM NFV (Fig. 4c), suggesting that the substitutions in NCA were compensatory for the replication of HIV-1 harboring protease and matrix of CL-4. However, CCAmt was outgrown by MA + PRmt in the absence of NFV, but its replication in the presence of 0.1 μM NFV was comparable with that of MA + PRmt under similar condition (Fig. 4d), suggesting that the substitutions in CCA reduced the replication capability of MA + PRmt, while NFV compensated the mutation effect. Sub-cloning analyses of proviral sequences at both of the passages 3 and 4 in competitive HIV-1 replication assay in the presence of 0.1 μM NFV showed that five of 10 clones were derived from CCAmt and the other five clones were derived from MA + PRmt, which confirmed that CCAmt and MA + PRmt had comparable replication ability in the presence of 0.1 μM NFV (Fig. 4d). MA + PRmt readily outgrew p17PRmt in the absence of NFV, but was outgrown by p17PR in the presence of 0.1 μM NFV (Fig. 4e), suggesting that the substitutions in NCA and CCA reduced the replication capability of MA + PRmt, while NFV counteracted the mutation effect and rather enhanced replication ability at sub-inhibitory concentration (Fig. 3, p17PRmt).

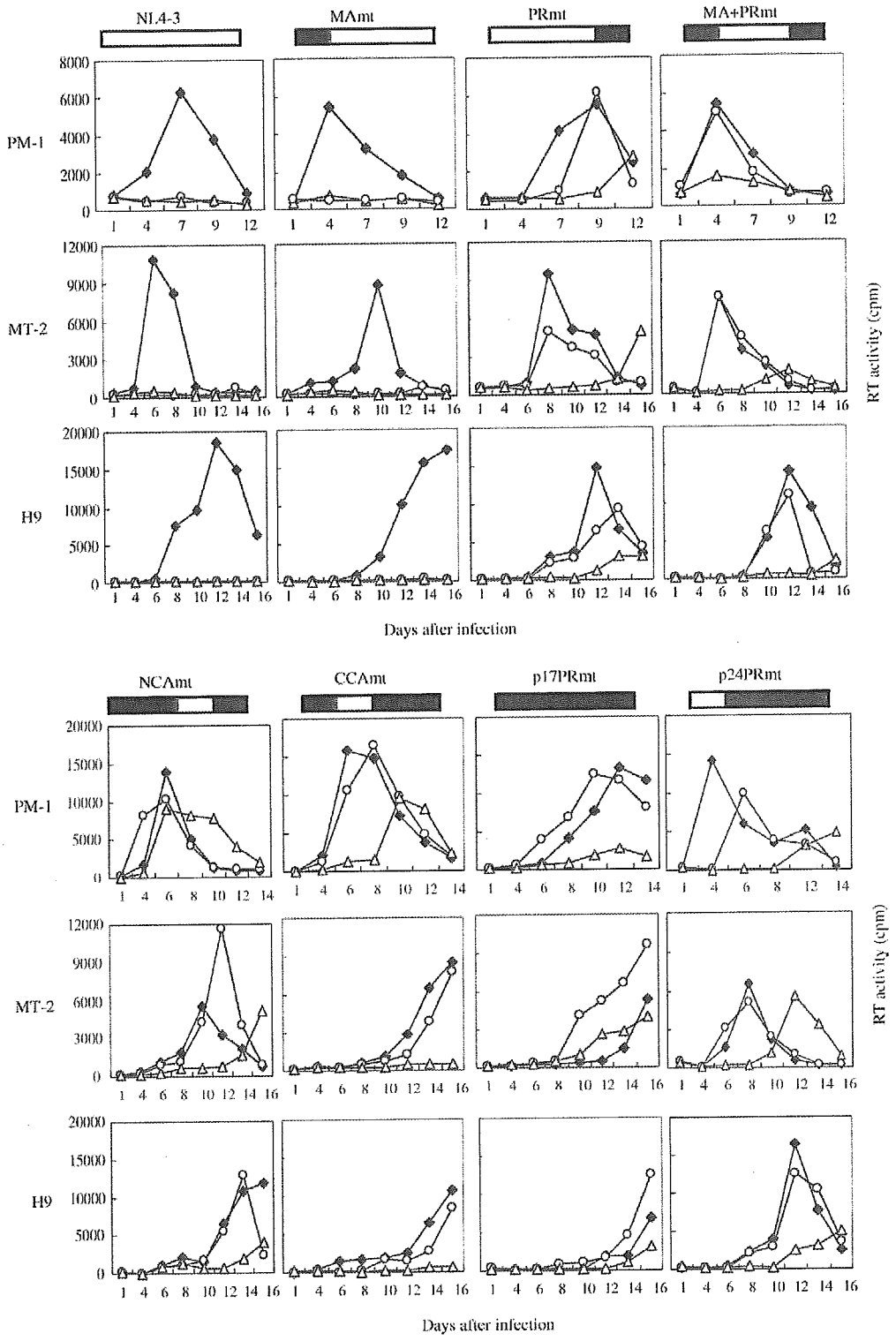

Fig. 3. Effects of NFV on replication capability of recombinant HIV-1s. PM-1, MT-2, and H9 cells (2×10^4 cells) were exposed to 0.2 ml of cell-free supernatant containing each HIV-1 clone (2×10^5 ^{32}P cpm of RT activity), washed once, and cultured in 0.2 ml of medium in the absence (closed diamonds) and presence of NFV (0.1 μM; open circles, 1 μM; open triangles). Half volume of the culture medium was changed every 2 or 3 days, and the supernatant was kept at −80 °C until the measurement of RT activity. Each experiment was carried out in duplicate and repeated three times, and representative data are shown.

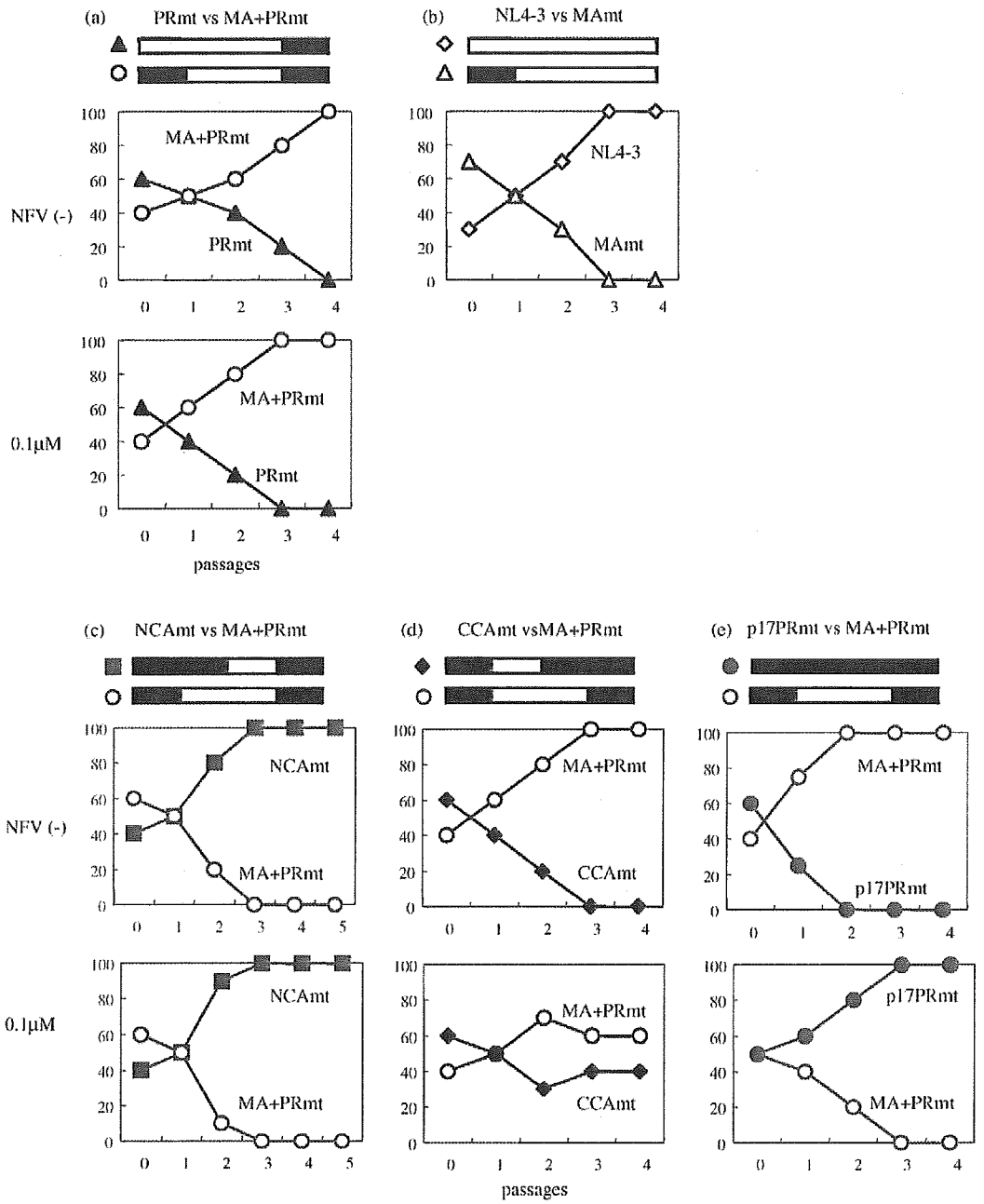

Fig. 4. One-to-one competitive HIV-1 replication assay. H9 cells (2×10^5 cells) were incubated with two recombinant HIV-1s (each of 100 $TCID_{50}$) simultaneously at 37 °C for 16 h, washed with PBS twice, and cultured in the absence and presence of 0.1 μM of NFV. At 7 days post-infection, the culture supernatant was used to infect fresh uninfected H9 cells. The cells harvested at each passage were subjected to direct DNA sequencing, and the viral population changes were determined by the relative peak height in the sequencing electrophoregram. The persistence of the original amino acid substitutions was confirmed for all infectious clones used in this assay. (a) PRmt vs. MA + PRmt; (b) NL4-3 vs. MAmt; (c) NCAmt vs. MA + PRmt; (d) CCAmt vs. MA + PRmt; (e) p17PRmt vs. MA + PRmt.

3.2. Gag substitutions conferring NFV resistance

To analyze the role of the substitutions in the matrix, NCA, and CCA in NFV resistance, IC_{50}s of NFV for the HIV-1 clones described above were determined by using MT-2 cells (Zhang et al., 1997). MAmt (IC_{50}: 9.4 nM) showed 1.9-fold resistance against NFV compared with NL4-3 (5.0 nM), and p17PRmt (893 nM) showed 3.3-fold resistance compared with p24PRmt (273 nM) (Table 1), indicating that the substitutions in the matrix may make a small contribution to the viral resistance against NFV. NCAmt (483 nM) had 2.1-fold resistance against NFV compared with MA + PRmt (229 nM), and p17PRmt had 4.1-fold resistance compared with CCAmt (217 nM), indicating that the substitutions in NCA gave positive impact on viral resistance. Interestingly, CCAmt showed 0.95-fold resistance against NFV compared with MA + PRmt, indicating that substitutions in CCA

Table 1
NFV resistance of recombinant HIV-1s

HIV-1	IC_{50} (nM)	Fold-resistance
NL4-3	5.0 ± 0.4	1.0
PRmt	241 ± 34	48
p24PRmt	273 ± 13	55
p17PRmt	893 ± 28	179
MAmt	9.4 ± 3.3	1.9
MA + PRmt	229 ± 21	46
NCAmt	483 ± 26	97
CCAmt	217 ± 32	43

The concentrations of drug added to the growth medium for calculation of the IC_{50}s were 0, 1, 3.16, 10, 31.6, 100, and 316 nM and 1 and 3.16 μM NFV, and the IC_{50}s were derived from plots of percent of inhibition of p24 production in culture supernatant versus NFV concentration.

may give small negative impact on viral resistance in the absence of the substitutions in NCA. p17PRmt, however, had 1.8-fold resistance compared with NCAmt, indicating the substitutions in CCA may give a small but positive contribution to viral resistance in the presence of the substitutions in NCA. The role of the substitutions in CCA in viral resistance was altered by the presence of the substitutions in NCA.

3.3. *Gag substitutions facilitating cleavage between matrix and capsid*

To further delineate the impact of each substitution, the Gag processing pattern was assessed in the absence and presence of NFV by Western blot analysis using anti-p24 monoclonal antibody (Fig. 5A1–2 and B1–2). As expected, 0.1 μM of NFV effectively blocked cleavage of the Gag p55 precursor of NL4-3 (percent density of p24; 4.7% versus 87.5% in Fig. 5A1; 4.2% versus 83.3% in Fig. 5A2). In contrast, NFV gave only a small influence on the cleavage patterns of the p55 precursor of MA + PRmt (percent density of p24; 65.5% versus 87.4% in Fig. 5A1; 77.8% versus 92.6% in Fig. 5A2), which is consistent with the indistinguishable replication kinetics of this mutant in the absence and presence of NFV (Fig. 3). Interestingly, NFV enhanced the cleavability of the p55 precursor of p17PRmt (percent density of p24; 94.8% versus 74.3% in Fig. 5A1; 72.2% versus 54.1% in Fig. 5A2), which was paralleled with NFV-dependent replication enhancement of this mutant (Fig. 3). NFV also gave a small positive effect on the cleavability of the p55 precursor of NCAmt (percent density of p24; 97.1% versus 94.6% in Fig. 5B1; 97.5% versus 96.2% in Fig. 5B2), which was paralleled with the partial enhancement of replication with NFV (Fig. 3). Furthermore, percent density of p24 of NCAmt was increased compared with that of MA + PRmt (percent density of p24; 94.6% and 96.2% versus 87.4% and 92.6% in the absence of NFV; 97.1% and 97.5% versus 65.5% and 77.8% in the presence of 0.1 μM NFV), suggesting that the substitutions in NCA play a significant role in Gag cleavability. Finally, NFV decreased percent density of p24 of CCAmt (percent density of p24; 68.9% versus 78.2% in Fig. 5B1; 45.3% versus 79.0% in Fig. 5B2), which was paralleled with NFV-induced delay of replication kinetics (Fig. 3). For further confirmation, the Gag processing pattern of NCAmt and CCAmt was also assessed by Western blot analysis using HIV-1-infected patient's serum (Fig. 5B3). As expected, NFV slightly increased cleavability of the p55 precursor of NCAmt (percent density of p24; 96.9% versus 94.5% in Fig. 5B3), and gave a negative impact on Gag cleavage of CCAmt (percent density of p24; 41.9% versus 74.3% in Fig. 5B3), which were well compatible with the cleavage pattern analyzed by using anti-p24 monoclonal antibody (Fig. 5B1, 2). In summary, NFV induced enhanced cleavability of Gag precursors of p17PRmt and NCAmt, which was well paralleled with NFV-induced enhancement of replication capability of these mutants.

4. Discussion

We previously reported that the substitutions in p6-protease segment alone are sufficient to confer NFV resistance while those in matrix are indispensable for the replication enhancement of CL-4 by NFV (Matsuoka-Aizawa et al., 2003). In the present study, we found that not only the matrix substitutions but the mutations in N-terminal half of capsid also played critical role in the enhancement and that the full potential of the enhancement phenotype was achieved only with the cooperation of mutations in the entire Gag and protease region of CL-4. The substitutions in matrix and those in N-terminal half of capsid compensated the otherwise compromised viral replication in the absence and presence of NFV (Fig. 4a and c). Probably, these substitutions cooperatively altered the tertiary structure of the Gag precursor and made the cleavage site between matrix and capsid more accessible to mutant protease harboring multiple resistance-associated mutations. The cleavage pattern analyzed by Western blot analysis supported the idea that the substitutions in N-terminal half of capsid improved the Gag cleavage. Percent density of p24 of NCAmt was increased compared with that of MA + PRmt in the absence of NFV (Fig. 5A1–2 and B1–2; 94.6% and 96.2% versus 87.4% and 92.6%). It is worth noting that CL-4 had a total of 56 amino acid substitutions in *gag-pro* genes compared with NL4-3; 22 substitutions had emerged during NFV-containing therapy, and 34 other substitutions had already existed before the introduction of the therapy, and that all the substitutions in N-terminal half of capsid of CL-4 were pre-existing before NFV-therapy (Fig. 1), suggesting that certain polymorphic amino acid residues seen in HIV-1 clinical isolates were associated with drug resistance. Interestingly, the amino acid insertion at the same site of the matrix of CL-4 compared with NL4-3 (Fig. 1; amino acids 121–125 in MA, QQAAA) was reported to increase viral replication harboring mutant protease by improving otherwise impaired Gag processing (Tamiya et al., 2004). Gatanaga et al. also reported that a polymorphic substitution in N-terminal half of capsid was indispensable for the development of high multitude of resistance against PIs (Gatanaga et al., 2002), though CL-4 did not harbor the same substitution. It is also known that certain drug-resistance-conferring amino acid substitutions found in one subtype HIV-1 isolated from patients under therapy may be detected in HIV-1 of other subtypes from untreated individuals (Cornelissen et al., 1997; Quinones-Mateu et al., 1998). More-

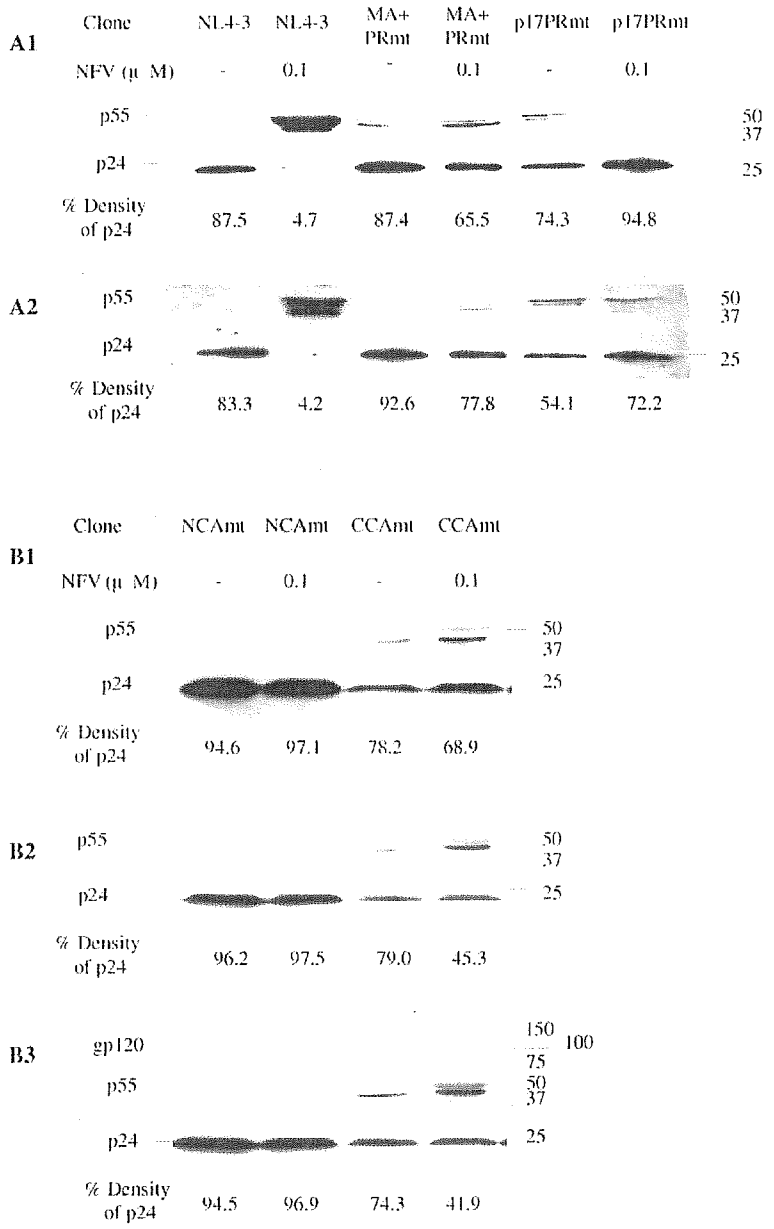

Fig. 5. Western blot analysis in the absence and presence of NFV. HeLa cells were transfected with each of full-length molecular clones and cultured in the absence and presence of 0.1 μM NFV. At 48 h post-transfection, virions in the culture supernatant (6×10^5 cpm of RT activity) were harvested and subjected to Western blot analysis. Gag proteins were visualized by using anti-p24 monoclonal antibody (A1-2, B1-2) and HIV-1-infected patient's serum (B3). Percent density of p24 was calculated as 100 × (p24 signal density/total Gag product signal densities) in a Western blot.

over, a recent study of Colson et al. revealed that HIV-2 strains harbor specific patterns of natural polymorphism and resistance (Colson et al., 2004). HIVs seem to acquire drug-resistance by utilizing the pre-existing polymorphic mutations and by coordinating the development of multiple substitutions.

Furthermore, the substitutions in N-terminal half of capsid of CL-4 altered the effect of NFV on viral replication. Sub-inhibitory concentration (0.1 μM) of NFV slightly accelerated the Gag precursor cleavage of NCAmt (percent density of p24; 97.1% versus 94.6% in Fig. 5B1; 97.5% versus 96.2% in Fig. 5B2; 96.9% versus 94.5% in Fig. 5B3), which was paralleled with the partial replication enhancement with NFV (Fig. 3), though it showed inhibitory effect in Gag processing of MA + PRmt (percent density of p24; 65.5% versus 87.4% in Fig. 5A1; 77.8% versus 92.6% in Fig. 5A2). Therefore, one of the mechanisms of viral replication enhancement with NFV is the improved processing of Gag harboring the substitutions in N-terminal half of capsid of CL-4 cooperated with the substitutions in the matrix. On the other hand, the role of the substitutions in C-terminal half of capsid seemed different, though they were also indispensable for the full potential of replication enhancement with NFV. They impaired the cleavability of Gag precursor

of MA + PRmt (Fig. 5A1–2 and B1–2; percent density of p24; CCAmt versus MA + PRmt = 78.2% and 79.0% versus 87.4% and 92.6%) and NCAmt (Fig. 5A1–2 and B1–2; percent density of p24; p17PRmt versus NCAmt = 74.3% and 54.1% versus 94.6% and 96.2%) in the absence of NFV, which were parallel with viral replication data (CCAmt versus MA + PRmt, Fig. 4d; p17PRmt versus NCAmt, Fig. 3). The effects of NFV on Gag cleavage pattern were different between CCAmt and p17PRmt; sub-inhibitory concentration (0.1 μM) of NFV facilitated the Gag cleavability of p17PRmt (percent density of p24; 94.8% versus 74.3% in Fig. 5A1; 72.2% versus 54.1% in Fig. 5A2), though it decreased the cleavability of CCAmt Gag (percent density of p24; 68.9% versus 78.2% in Fig. 5B1; 45.3% versus 79.0% in Fig. 5B2; 41.9% versus 74.3% in Fig. 5B3), which was also parallel with viral replication data showing enhancement only in p17PRmt but not in CCAmt (Fig. 3). Considering together, the substitutions in C-terminal half of capsid compromised viral replication by impairing the Gag preprocessing, and NFV could counteract the negative impact only in the presence of the substitutions in N-terminal half of capsid. In the absence of the substitutions in N-terminal half of capsid, only partial counteraction was seen (Fig. 4d). In summary, NFV-induced viral replication enhancement of CL-4 was caused by two mechanisms; NFV facilitates the processing of Gag harboring the substitutions in the matrix and N-terminal half of capsid of CL-4, and NFV counteracts the impaired Gag cleavage caused by the substitutions in C-terminal half of capsid of CL-4 only in the presence of the substitutions in the matrix and N-terminal half of capsid of CL-4. Therefore, the full potential of the enhancement phenotype was achieved only with the cooperation of mutations in the entire Gag and protease region of CL-4.

Notably, we found several other PI-resistant isolates with the phenotype of PI-dependent replication enhancement (data not shown), suggesting that HIV-1 can evolve to acquire capability to replicate better with the drugs. Such replication enhancement with antiretroviral agents presents formidable challenge in the therapy of HIV-1 infection. Future studies of structural analyses of Gag precursor(s) harboring substitutions of these mutants are warranted to clarify the underlying mechanism(s).

Acknowledgments

The authors thank A. Hachiya, K. Tsuchiya, Y. Suzuki, and Y. Hirabayashi for their helpful suggestions and continuous discussions throughout this study. We are also indebted to Y. Takahashi and F. Negishi for their technical assistance. This study was supported by a Grant-in-Aid for AIDS Research from the Ministry of Health, Labor, and Welfare of Japan (H15-AIDS-001), by the Organization of Pharmaceutical Safety and Research (01-4), and by the Japanese Foundation for AIDS Prevention.

References

Bleiber, G., Munoz, M., Ciuffi, A., Meylan, P., Telenti, A., 2001. Individual contributions of mutant protease and reverse transcriptase to viral infectivity, replication, and protein maturation of antiretroviral drug-resistant human immunodeficiency virus type 1. J. Virol. 75, 3291–3300.

Colson, P., Henry, M., Tourres, C., Lozachmeur, D., Gallais, H., Gastaut, J.A., Moreau, J., Tamalet, C., 2004. Polymorphism and drug-selected mutations in the protease gene of human immunodeficiency virus type 2 from patients living in southern France. J. Clin. Microbiol. 42, 570–577.

Cornelissen, M., van den Burg, R., Zorgdrager, F., Lukashov, V., Goudsmit, J., 1997. pol gene diversity of five human immunodeficiency virus type 1 subtypes: evidence for naturally occurring mutations that contribute to drug resistance, limited recombination patterns, and common ancestry for subtypes B and D. J. Virol. 71, 6348–6358.

Croteau, G., Doyon, L., Thibeault, D., McKerche, G., Pilote, L., Lamarre, D., 1997. Impaired fitness of human immunodeficiency virus type 1 variants with high-level resistance to protease inhibitors. J. Virol. 71, 1089–1096.

Doyon, L., Croteau, G., Thibeault, D., Poulin, F., Pilote, L., Lamarre, D., 1996. Second locus involved in human immunodeficiency virus type 1 resistance to protease inhibitors. J. Virol. 70, 3763–3769.

Gatanaga, H., Suzuki, Y., Tsang, H., Yoshimura, K., Kavlick, M.F., Nagashima, K., Gorelick, R.J., Mardy, S., Tang, C., Summers, M.F., Mitsuya, H., 2002. Amino acid substitutions in Gag protein at non-cleavage sites are indispensable for the development of a high multitude of HIV-1 resistance against protease inhibitors. J. Biol. Chem. 277, 5952–5961.

Kosalaraksa, P., Kavlick, M.F., Maroun, V., Le, R., Mitsuya, H., 1999. Comparative fitness of multi-dideoxynucleoside-resistant human immunodeficiency virus type 1 (HIV-1) in an *in vitro* competitive HIV-1 replication assay. J. Virol. 73, 5356–5363.

Martinez-Picado, J., Savara, A.V., Sutton, L., D'Aquila, R.T., 1999. Replicative fitness of protease inhibitor-resistant mutants of human immunodeficiency virus type 1. J. Virol. 73, 3744–3752.

Matsuoka-Aizawa, S., Sato, H., Hachiya, A., Tsuchiya, K., Takebe, Y., Gatanaga, H., Kimura, S., Oka, S., 2003. Isolation and molecular characterization of a nelfinavir (NFV)-resistant human immunodeficiency virus type 1 that exhibits NFV-dependent enhancement of replication. J. Virol. 77, 318–327.

Quinones-Mateu, M.E., Albright, J.L., Mas, A., Soriano, V., Arts, E.J., 1998. Analysis of pol gene heterogeneity. Viral quasispecies, and drug resistance in individuals infected with group O strains of human immunodeficiency virus type 1. J. Virol. 72, 9002–9015.

Tamiya, S., Mardy, S., Kavlick, M.F., Yoshimura, K., Mistuya, H., 2004. Amino acid insertions near Gag cleavage sites restore the otherwise compromised replication of human immunodeficiency virus type 1 variants resistant to protease inhibitors. J. Virol. 78, 12030–12040.

Turner, B.G., Summers, M.F., 1999. Structural biology of HIV. J. Mol. Biol. 285, 1–32.

Zhang, Y.M., Imamichi, H., Imamichi, T., Lane, H.C., Falloon, J., Vasudevachari, M.B., Salzman, N.P., 1997. Drug resistance during indinavir therapy is caused by mutations in the protease gene and in its Gag substrate cleavage sites. J. Virol. 71, 6662–6670.

ABSTRACT 106

Antiviral Therapy 2005; 10:S116

Analysis of interference and co-evolution between protease inhibitor resistant mutations and *gag* mutations

T Ueda, L Myint, T Shiino, M Nishizawa, M Matsuda, W Sugiura

National Institute of Infectious Diseases, Tokyo, Japan

OBJECTIVE: To better understand the mechanism of evolution of drug-resistant HIV-1, we analysed the interference between protease inhibitor (PI) resistant mutations and *gag* mutations both statistically and virologically.

METHODS: HIV-1 patient samples were collected during the period April 1997 to June 2004. HIV-1 RNA was extracted from 200μl of plasma, and 1909bps gag-protease fragment was amplified by RT-PCR. Sequences were analyzed using ABI-3100, and mutation points were determined through comparison with HXB2. Linkage-disequilibrium between the PI-resistant mutations and the *gag* mutations was calculated, and the significance of each disequilibrium value was defined by τ test. Representative recombinant virus clones were constructed, and their *gag* processing patterns and fitness were evaluated.

RESULTS: One hundred and forty-four cases (118 subtype B and 26 CRF01_AE) were examined in the study. Of these, 46 were treatment naive, 95 had exposure to anti-retrovirals, and in three cases no treatment information was obtained. To maintain statistical accuracy, PI resistant mutations found in more than five patients were selected for disequilibrium analysis. Subtype B samples matching this criteria were L10I (n=25), D30N (n=10), M36I (n=31), M46I (n=16), I54V (n=10), V82A (n=10), N88D (n=6), N88S (n=5) and L90M (n=17). Five mutations within *gag* cleavage sites demonstrated significant disequilibrium (P<0.001) with certain PI resistant mutations. These were (i) Y132FGag (p17/p24) with V82APR, L90MPR and I54VPR; (ii) I376V (p2/p7) with L90MPR; (iii) A431VGag (p7/p1) with M46IPR, V82APR, L10IPR and I54VPR; (iv) L449V/PGag (p1/p6) with L90MPR and M36IPR; and (v) R452KGag (p1/p6) withD30NPR and N88DPR. Among these, Y132FGag was newly identified as a PI resistance related mutation. Due to the small number of cases examined, no significant site was identified in CRF01_AE cases. We constructed recombinant viruses with Y132FGag or A431VGag, and confirmed that these cleavage site mutations affected virus fitness and *gag* processing.

CONCLUSION: Our study confirmed distinct evolutional interference between PI resistant mutations and *gag* sequences. We identified that the Y132FGag mutation may interfere with V82APR, L90MPR and I54VPR PI resistant mutations. Our results give a better understanding of the HIV drug resistance evolution pathway, and may be beneficial to the design of custom-made treatment protocols.

ABSTRACT 104

Antiviral Therapy 2005; 10:S114

Inference of evolutionary forces driving HIV-1 drug-resistance acquisition under HAART using longitudinal HIV-1 protease gene samples

N Hasegawa[1], W Sugiura[2], M Matsuda[2], K Mogushi[1], H Tanaka[1] and F Ren[3]

[1]Department of Computational Biology
[3]Center for Information Medicine, Tokyo Medical and Dental University, Tokyo
[2]AIDS Research Center, National Institute of Infectious Diseases, Tokyo, Japan

OBJECTIVES: To clarify possible mechanisms of HIV-1 drug-resistance acquisition, we developed a computational algorithm for inferring within-host evolutionary process and applied the algorithm to a longitudinal data set of HIV-1 protease sequences (189 clones) collected from a single patient under HAART over three years.

METHODS: We calculated genetic distances between viral variants at two adjacent sampling time points: Tn and Tn+1, converted these distances into rank-order and calculated their rank correlation coefficients. We then used the correlations to cluster these viral variants with correlation coefficient above 0.7. By connecting viral variants at adjacent time points with shortest genetic distance, we identified the pathways of viral evolution and constructed a longitudinal phylogenetic tree. We then estimated the synonymous (dS) and non-synonymous (dN) substitution rates for escaped variants as indicators of viral fitness and of selective pressures exerted on the virus by antiretroviral treatment.

RESULTS: The reconstructed phylogenetic tree showed two major viral subpopulations, sP1 and sP2, prevailed during the study period. The sP1 had two unique mutations, D30N and N88D, and was the dominating subpopulation when the patient was treated with nelfinavir, but disappeared with discontinuation of nelfinavir. The sP2 possessed two unique mutations, G73S and L90M. The sP2 had become a dominant subpopulation when the treatment switched from nelfinavir to saquinavir+ritonavir. By estimating nucleotide substitution rates, we found that the sP1 showed high dN immediately after initiation of nelfinavir, while the sP2 showed higher dS mostly during the observation period.

CONCLUSIONS: We found two main features concerning HIV-1 drug-resistance acquisition. First, our results strongly support that D30N and L90M are mutually exclusive during the evolutionary process. Second, the selective pressure exerted on the virus is highly variable over time when different drugs are administered. We obtained estimates of dN/dS>1 in the sP1, suggesting that the virus was undergoing adaptive evolution when nelfinavir was administered, but the fitness of the sP1 might be lower than that of the sP2 as the latter showed higher dS that means the virus had a higher replication rate.

Antiviral Chemistry & Chemotherapy 16:363–373

A novel small molecular weight compound with a carbazole structure that demonstrates potent human immunodeficiency virus type-1 integrase inhibitory activity

Hua Yan[1], Tomoko Chiba Mizutani[1], Nobuhiko Nomura[2], Tadakazu Takakura[2], Yoshihiro Kitamura[3], Hideka Miura[1], Masako Nishizawa[1], Masashi Tatsumi[1], Naoki Yamamoto[1] and Wataru Sugiura[1*]

[1]AIDS Research Center, National Institute of Infectious Diseases, Tokyo, Japan
[2]Research and Discovery Laboratories, Toyama Chemical Co. Ltd., Toyama, Japan
[3]Division of Infectious Diseases, Advanced Clinical Research Center, Institute of Medical Science, University of Tokyo, Japan.

*Corresponding author: Tel: +81 42 561 0771; Fax: +81 42 561 7746; E-mail: wsugiura@nih.go.jp

The integration of reverse transcribed proviral DNA into a host genome is an essential event in the human immunodeficiency virus type 1 (HIV-1) replication life cycle. Therefore, the viral enzyme integrase (IN), which plays a crucial role in the integration event, has been an attractive target of anti-retroviral drugs. Several IN inhibitory compounds have been reported previously, yet none has been successful in clinical use. To find a new, more successful IN inhibitor, we screened a diverse library of 12 000 small molecular weight compounds randomly by *in vitro* strand-transfer assay. We identified a series of substituted carbazoles that exhibit strand-transfer inhibitory activity at low micromolar concentrations. Of these, the most potent compound exhibited an IC_{50} of 5.00 ±3.31 μM (CA-0). To analyse the structural determinants of strand-transfer inhibitory activity of the carbazole derivatives, we selected 23 such derivatives from our compound library and performed further analyses. Of these 23 compounds, six showed strong strand-transfer inhibition. The inhibition kinetics analyses and ethidium bromide displacement assays indicated that the carbazole derivatives are competitive inhibitors and not intercalators. An HeLa4.5/LTR-nEGFP cell line was employed to evaluate *in vitro* virus replication inhibition of the carbazole derivatives, and IC_{50} levels ranged from 0.48–1.52 μM. Thus, it is possible that carbazole derivatives, which possess structures different from previously-reported IN inhibitors, may become novel lead compounds in the development of IN inhibitors.

Keywords: integrase inhibitor, carbazole, HIV-1, antiretroviral drug

Introduction

Human immunodeficiency virus type 1 (HIV-1), causative agent of acquired immunodeficiency syndrome (AIDS), possesses three critical enzymes for replication. These are protease (PR), reverse transcriptase (RT), and integrase (IN) (Ruscetti, 1985; Kohl *et al.*, 1988; LaFemina *et al.*, 1992). As inactivating any of these enzymes may negate the infectivity of HIV-1, the enzymes have been targets of anti-retroviral drug development. Indeed, great progress in anti-retroviral drug discovery has been achieved in recent decades, and today 10 RT inhibitors and eight PR inhibitors (De Clercq, 1992; Tronchet & Seman, 2003; Balzarini, 2004; Imamichi, 2004) are available for anti-retroviral treatments. The third enzyme, IN, has also been a major target of inhibitor development. L-708,906 and L-731,988, which possess diketo acid moieties within their structures, were the first IN-specific inhibitors discovered (Pommier *et al.*, 2000; Dayam & Neamati, 2003; Pluymers *et al.*, 2002; Hazuda *et al.*, 2000). S-1360 and L-870,810, which also have diketo acid moieties, are IN inhibitors that have reached clinical Phase I/II trials for the first time (Johnson *et al.*, 2004; Hazuda *et al.*, 2004). However, although there have been large advances in the development of IN inhibitors, further research and analysis is required to develop clinically usable compounds.

Integrase (IN), the leading target of novel anti-retroviral inhibitor development, is the enzyme responsible for integration, wherein reverse transcribed HIV-DNA is inserted into a host genome, and is critical for viral replication, which in turn establishes latency and chronic infection (Chun *et al.*, 1995). IN is composed of three distinct

domains – the N-terminal domain (amino acids 1–50) with a zinc-binding motif (Schauer & Billich, 1992; Burke *et al.*, 1992), the catalytic core domain (amino acids 50–212) with polynucleotidyl transfer activity and sequence-specific endonuclease activity (Engelman & Craigie, 1992; Engelman *et al.*, 1994) and the C-terminal domain (amino acids 212–288), which has been thought to relate to nonspecific DNA binding (Khan *et al.*, 1991; Woerner & Marcus-Sekura, 1993).

At present, the function and structure of each domain has not been fully understood. The most well-analysed domain is the catalytic core domain, and its active site has highly conserved amino acidic residues Asp64, Asp116 and Glu152, which are critical for polynucleotidyl transfer activity (LaFemina *et al.*, 1992; Engelman *et al.*, 1995). Previously reported potent IN inhibitors L-708,906, L-731,988, L-801,810, S-1360 and 5-CITEP are all targeted to this domain. These inhibitors bind to the active site, displace divalent metal ion Mg^{2+} from the active site and inactivate the catalytic activity of IN (Grobler *et al.*, 2002; Dayam & Neamati, 2003; Goldgur *et al.*, 1999; Johnson *et al.*, 2004). No specific inhibitors have been reported for the N-terminal and C-terminal domains.

In the present study we attempted to identify novel IN inhibitory compounds, and therefore we conducted a random screening of a library of small molecular weight compounds. As a result, we discovered a series of novel IN inhibitory compounds with carbazole structures, that are quite different from previously reported inhibitory compounds.

Materials and methods

Preparation of integrase

The sequence coding the NL4-3 integrase (IN) was cloned into pET28b(+) (Novagen, Madison, WI, USA), generating pET-IN that codes NL4-3 IN with a hexa-histidine tag at the N-terminus. *Escherichia coli* strain Rosetta (DE3) (Novagen) transformed with pET-IN was grown in 1 l of Super Broth (Biofluids, Camarillo, CA, USA) containing 100 μg/ml kanamycin at 30°C until the optical density of the culture had reached between 0.5 and 0.7 at 600 nm. The recombinant protein expression was induced by isopropyl-1-thio-D-galactopyranoside. After incubation for 3 h, the cells were harvested and resuspended in 100 ml of preparation buffer (20 mM Tris-HCl, pH 8.0, 0.5 M NaCl) and disrupted by sonication. Following high-speed centrifugation at 40 000×g for 45 min at 4°C, the pellet was homogenized in GBB buffer (50 mM Tris-HCl, pH 8.0, 6 M Guanidine HCl and 2 mM 2-ME). The residual pellet was again sonicated and centrifuged at 40 000×g for 30 min at 4°C.

The supernatant was filtered through a 0.22 μm filter and mixed with 1 ml of nickel-affinity resin (Sigma, St. Louis, MO, USA), and incubated overnight at 4°C. The resin was washed twice by mixing with 20 ml of GBB containing 5 mM imidazole (Sigma). The protein was eluted with GBB containing 1 M imidazole. The fractions containing integrase were pooled and 0.5 M EDTA was added to a final concentration of 5 mM. This eluted protein was then sequentially dialysed against (i) 6 M guanidine HCl, 50 mM Tris-HCl (pH 8.0), 2 mM 2-ME, 1 mM EDTA for 2 h at room temperature, (ii) 6 M guanidine HCl, 50 mM Tris-HCl (pH 8.0), 10 mM DTT, 1 mM EDTA for 16 h at room temperature, (iii) 4 M urea, 50 mM Tris-HCl (pH 8.0), 0.5 M NaCl, 1 mM DTT, 0.1 mM EDTA for 16 h at 4°C, (iv) 2 M urea, 50 mM Tris-HCl (pH 8.0), 0.5 M NaCl, 1 mM DTT, 0.1 mM EDTA, 20% (w/v) glycerol for 16 h at 4°C, (v) 1 M urea, 50 mM Tris-HCl (pH 8.0), 1 M NaCl, 1 mM DTT, 0.1 mM EDTA, 15 mM 3-[(3-cholamidopropyl) dimethylammonio]-1-propanesulfonate (CHAPS), 20% (w/v) glycerol for 16 h at 4°C, and (vi) 50 mM Tris-HCl (pH 8.0), 1 M NaCl, 1 mM DTT, 0.1 mM EDTA, 15 mM CHAPS, 20% (w/v) glycerol for 16 h at 4°C. The final preparation was stored at −80°C.

The purified enzyme activity was confirmed and evaluated by strand-transfer assay using M8 apparatus (IGEN, Gaithersburg, MD, USA).

Preparation of test compounds

A diverse library of 12 000 small-molecule compounds was supplied by Toyama Chemicals Co. Ltd. (Toyama, Japan). All test compounds were dissolved in DMSO and adjusted to 2 mM concentration. S-1360 was synthesized as positive control for strand transfer assay.

Construction of strand-transfer assay

Two different strand-transfer assay systems were employed in the IN inhibitor screening trial. For the first screening step, an M8 apparatus and strand-transfer assay kit, ORIGEN HIV integrase assay (IGEN), was used. In brief, magnetic beads coated with 29 mer donor double-stranded DNA (dsDNA) were mixed with purified IN (15 pmol), followed by adding the test compound and 20 mer target dsDNA tagged with ruthenium, conducting electronically inducible fluorescence chemistry, and incubating for 1 h at 37°C. Subsequently, the entire reaction solution was applied to the M8 apparatus, and then strand-transfer products were captured by a magnet in the flow-circuit of the equipment. The amount of the strand-transfer product was measured by ruthenium fluorescence activity. For the second and later screening steps, in-house strand-transfer assay was employed. The in-house assay was designed in 96-well plate format to achieve high-throughput screening.

The following donor and target DNA oligonucleotides were designed and used:
Donor-1 (D1): 5′-ACTGCTAGAGATTTTCCACACTGACTAAAAG-3′
Donor-2 (D2): Biotin-5′-CTTTTAGTCAGTGTGGAAAATCTCTAGCA-3′
Target-1 (T1): 5′-CTAGAGATTTTCCACACTGACTAAAAG-3′-Digoxigenin (DIG),
Target-2 (T2): 5′-CTTTTAGTCAGTGTGGAAAATCTCTAG-3′-DIG

To form dsDNA, the D1–D2 pair and the T1–T2 pair were mixed in the presence of 0.1 M NaCl and denatured for 10 min at 95°C, followed by an annealing process, gradual cooling down to room temperature. One pmol biotinulated donor dsDNA (D1–D2), 15 pmol IN protein and 5 μl test compounds (100 μM in DMSO) were mixed together in assay buffer (25 mM 3-(N-morpholino)-propanesulfonic acid, pH 7.2, 25 mM NaCl, 10 mM $MgCl_2$, 10 mM DTT, 5% PEG, 10% DMSO), followed by the addition of 0.75 pmol target dsDNA (T1–T2), and adjusted to a final volume of 100 μl and incubated for 1 h at 37°C. After the incubation, the mixture was adjusted to a final volume of 200 μl with ELISA buffer (20 mM Tris [pH 8.0], 0.4 M NaCl, 10 mM EDTA, 0.1 mg/ml sonicated DNA). To harvest the strand-transfer product, the mixture was transferred into a 96-well micro titre plate coated with streptavidin (PIERCE, Rockford, IL, USA), followed by adding an alkaline phosphatase conjugated anti-DIG antibody (Roche Diagnostics, Mannheim, Germany) and a disodium 3-(4-methoxyspiro{1,2-dioxetane-3,2′-(5′-chloro)tricyclo[3.3.1.1^{3,7}]decan}-4-yl) phenyl phosphate (CSPD) substrate (Roche). The lumino-intensity was quantified with a Luminous CT-9000D luminometer (DIA-IATRON, Tokyo, Japan).

In addition to the above two different strand-transfer assays, a strand-transfer assay with radioisotope labelled target DNA and SDS-PAGE was employed in order to visually confirm the strand-transfer inhibition (Craigie *et al.*, 1995). By use of T4 polynucleotide kinase (TAKARA BIO, Osaka, Japan), the 5′ end of 20 mer target oligonucleotide-A (5′-TGTGGAAAATCTCTAGCAGT-3′) was labelled with [γ-^{32}P] ATP (370 MBq/μl, Amersham Bioscience, Tokyo, Japan). After the labelling reaction was terminated by adding EDTA, complementary oligonucleotide-B (5′-ACTGCTAGAGATTTTCCACA-3′) was added, and dsDNA was formed by heat denaturation and gradual cooling to room temperature. Unincorporated [γ-^{32}P]ATP was removed by G-25 Column (Amersham Bioscience, Piscataway, NJ). The reaction products were applied to 20% denatured polyacrylamide gel electrophoresis (300V/25A). The result of the electrophoresis was analysed by BAS-2500 (Fuji film, Tokyo, Japan).

Inhibition kinetics of IN

To analyse the strand-transfer inhibition mechanism of the test compounds, whether the action is competitive inhibition or non-competitive inhibition, Michaelis-Menten constant (K_m) and maximum velocity (V_{max}) were evaluated. Strand-transfer inhibition was evaluated on eight different time points (0, 1, 3, 5, 7.5, 10, 15, and 20 min) with four different compound concentrations (0, 1, 5, 10 μM) and target DNA concentrations (0.167, 0.25, 0.5, and 1 pmol). The initial reaction rate constants of IN were determined by linear regression using linear data points of product concentration–time plots. K_m and V_{max} were calculated from the Y-axis intercept in a plot of the slopes of Lineweaver-Burk analysis.

Intercalative activity evaluation

To clarify the possibility of intercalative activity of test compounds, ethidium bromide (EtBr) displacement assay was carried out following the protocol reported previously (Cain *et al.*, 1978). In brief, 1 μM calf thymus DNA (Invitrogen, Carlsbad, CA, USA) was mixed with EtBr (final concentration at 1.26 μM) and reaction buffer (2 mM HEPES, 10 μM EDTA, 9.4 mM NaCl, pH 7.0), and incubated for 10 min at room temperature. After the incubation, test compounds were added into the calf thymus DNA–EtBr mixture at different concentrations (final concentrations of 0.01–1000 μM). Fluorescence intensity of each mixture was determined by Fluoroskan Ascent FL (Helsinki, Finland. Excited at 544 nm, emitted at 590 nm). Actinomycin D (ICN Biomedical, Aurora, OH, USA), which is known as an intercalator, was employed as the positive control of the assay.

Molecular modelling studies

Molecular modelling studies were carried out using SYBYL software Version 6.9.1 (Tripos, St. Louis, MO, USA) running on an SGI Fuel workstation equipped with 600-MHz R14000 processor (SGI, Mountain View, CA, USA).

Evaluation of *in vitro* antiviral activity.

To evaluate HIV-1 replication inhibition by selected test compounds, *in vitro* antiviral assays were performed using a HeLa4.5/nEGFP reporter cell line. The HeLa4.5/nEGFP reporter cell line was established by transfection of CD4 and LTR driven EGFP reporter protein into the HeLa cell line. HeLa4.5/nEGFP reporter cells were maintained with D-MEM (Sigma) containing 5% FCS (Hyclone, Logan, UT, USA), 500 μg/ml G418, 1 μg/ml blasticidin and 2 μg/ml puromycin.

One day before conducting the assay, $1x10^4$ HeLa4.5/nEGFP cells were seeded into clear bottom black 96-well plates (NUNC, Rochester, NY, USA) with

200 μl/well medium and incubated at 37°C, 5% CO_2. The next day, 1250 $TCID_{50}$ HXB2 were added in each well, followed by addition of the test compounds in final concentrations of 5, 1, 0.2, 0.04, 0.008, 0.0016, 0.00032, and 0.000064 μM. Forty-eight hours after infection, the cells were fixed by 3.2% formaldehyde and the nuclei of cells were stained by 10 μg/ml Hoechst33342 (Molecular Probes, Engene, OR, USA). EGFP positive cell number ($EGFP^+$) and Hoechst33342 positive cell number ($hoechst33342^+$) were determined by Cellomics Array Scan, HSC Systems (Beckman Coulter, Tokyo, Japan).

Inhibitory activity of each compound was determined by the following formula:

% inhibition = 1 − {($EGFP^+$ cell number with drug/$hoechst33342^+$ cell number with drug) − ($EGFP^+$ cell number without infection/$hoechst33342^+$ cell number without infection)}/{($EGFP^+$ cell number without drug/$hoechst33342^+$ cell number without drug) − ($EGFP^+$ cell number without infection/$hoechst33342^+$ cell number without infection)}.

Results

A small molecule bearing a carbazole moiety demonstrated strand-transfer inhibitory activity

A diverse library of 12 000 small-molecule compounds was screened for strand-transfer inhibitory activity at 100 μM concentration by M8 apparatus. Seventy-two compounds that demonstrated more than 80% strand-transfer-inhibition were selected and applied to the second screening using in-house strand-transfer assay. In the second screening, to confirm dose-dependent inhibition of the test compounds, each compound was tested at four different concentrations. Of the 72 compounds, a compound bearing a carbazole moiety, 8-chloro-2-[2-(dimethylamino)ethyl]-9-hydroxy-5-methylpyrrolo[3,4-c]carbazole-1,3(2H,6H)-dione (coded as **CA-0**), was found to demonstrate potent strand-transfer inhibitory activity (Figure 1A). As shown in Figure 1B, **CA-0** demonstrated clear dose-dependent inhibition of the strand-transfer reaction with an IC_{50} of 5.00 ±3.31 μM. The dose-dependent inhibition was also confirmed by SDS-PAGE with [γ-^{32}P] labelled target DNA. As demonstrated in Figure 1C, strand-transferred product bands diminished along with increased concentration of the inhibitor. IC_{50} value determined from intensities of the bands was 1.24 ±0.09 μM, which was consistent with that evaluated via the plate assay.

Strand-transfer inhibition of 23 carbazole derivatives, and the relationship between their structures and inhibitory activity

To understand the relationship between structure and strand-transfer inhibition activity, we selected 23 carbazole

Figure 1. Structure and strand transfer inhibitory activity of 8-chloro-2-[2-(dimethylamino) ethyl]-9-hydroxy-5-methylpyrrolo[3,4-c]carbazole-1,3(2H,6H)-dione (**CA-0**)

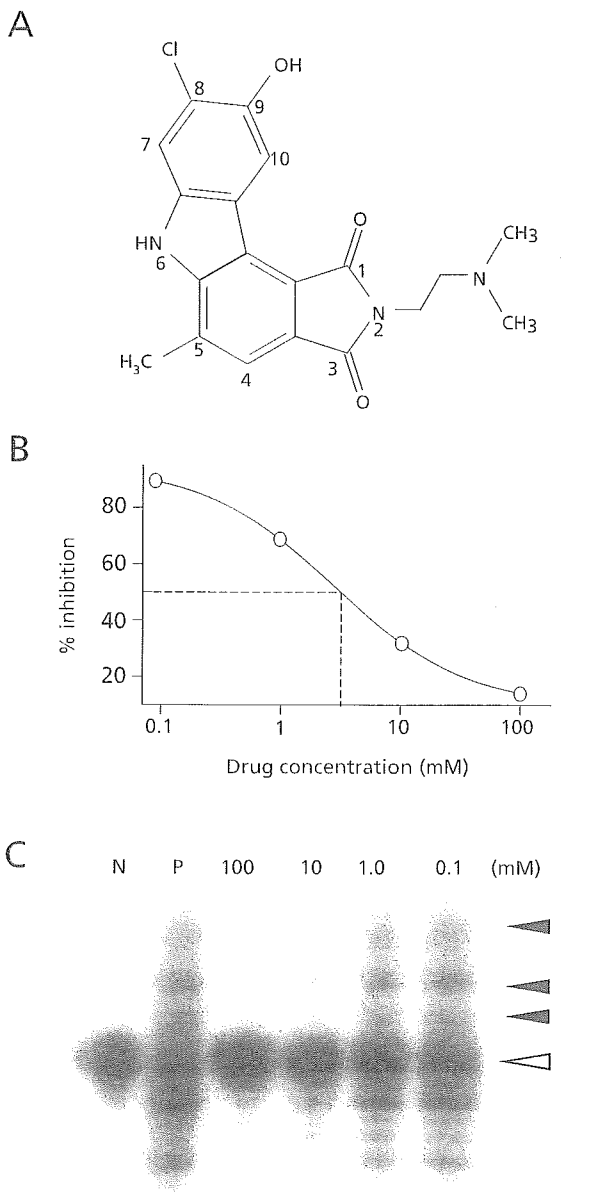

(A) The structure of **CA-0**, a strand transfer inhibitory compound identified from among a library of 12 000 small molecular weight compounds. It has a carbazole structure as a scaffold. The small numbers written beside the structure indicate the residue number of the compound. **(B)** A dose–response curve of **CA-0**. The dotted line indicates the IC_{50} point of the chemical, which was 5.00 ±3.31 μM. **(C)** A strand transfer assay by radioisotope-labelled oligonuceotide. Lane 1 "N" stands for the negative control, with only a radioisotope-labelled nucleotide. Lane 2 "P" stands for positive control, with radioisotope-labelled nucleotide and recombinant integrase. Lanes 3 to 6 were with inhibitor. The open triangle and solid triangle indicate labelled oligonucelotide and strand transfer products, respectively.

derivatives with different substituents. As demonstrated in Figure 2, all compounds had pyrrolo[3,4-c]carbazole structures as scaffolds, and all except **CA-5**, **CA-10** and **CA-19** had 2-dimethylaminoethyl group at position R2. Six of the 23 compounds demonstrated potent strand-transfer inhibition comparable to that of **CA-0**. These compounds were **CA-1**, **CA-4**, **CA-8**, **CA-9**, **CA-12** and **CA-13**. IC_{50} values of these test compounds were similar with positive control S-1360. Moderate inhibitory activities were observed in twelve compounds, **CA-2**, **CA-3**, **CA-7**, **CA-11**, **CA-14**, **CA-15**, **CA-16**, **CA-17**, **CA-18**, **CA-21**, **CA-22** and **CA-23**. Five compounds, **CA-5**, **CA-6**, **CA-10**, **CA-19** and **CA-20**, did not show significant inhibition, even at the highest concentration tested

Figure 2. Structures of **CA-0** and 23 carbazole derivatives evaluated for strand transfer inhibitory activity

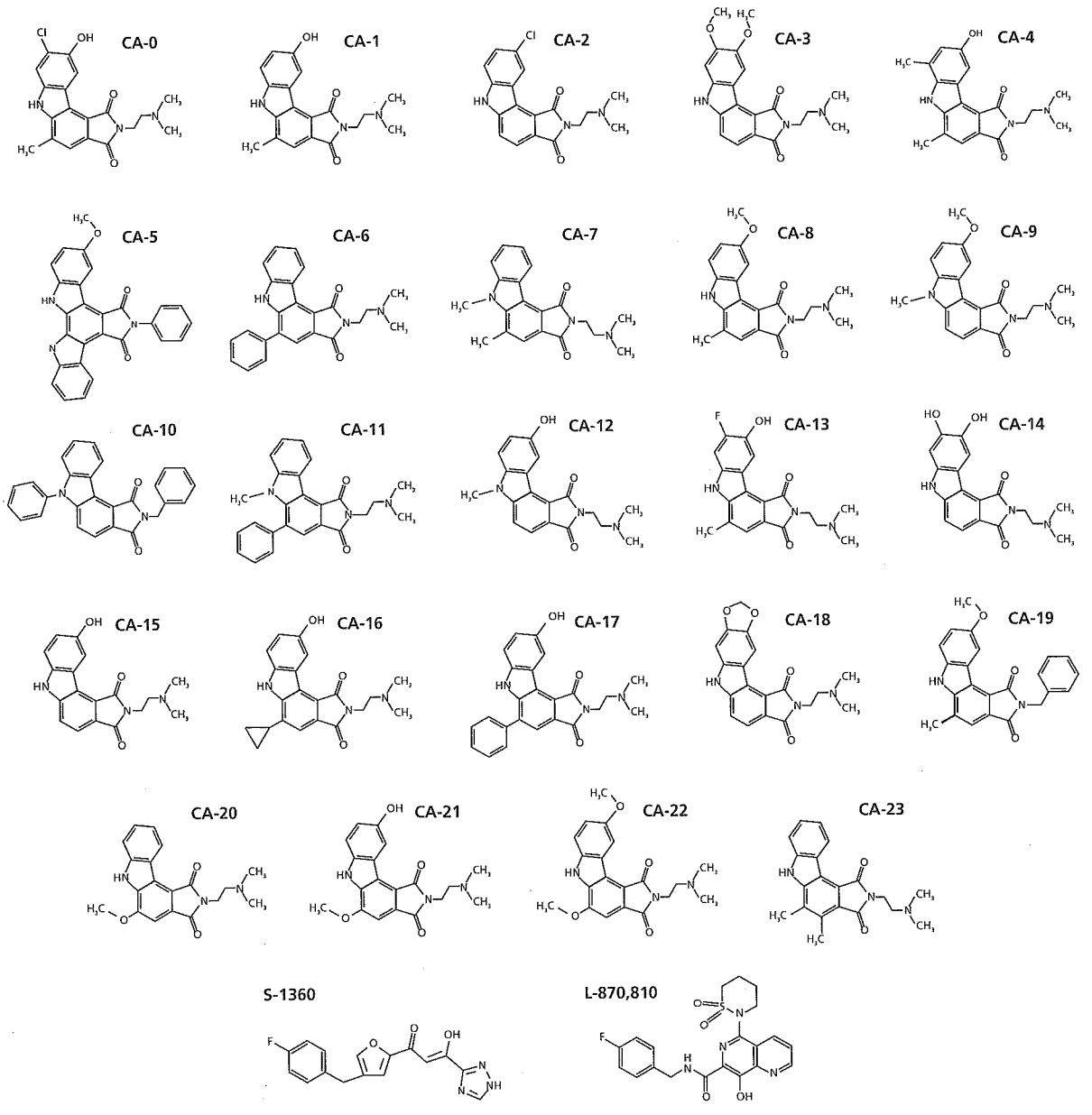

CA-0 and 23 related compounds with carbazole scaffold tested for strand-transfer inhibitory activities are depicted. S-1360 and L-870,810, which have previously been reported as potent IN inhibitors, are also shown.

(100 μM). The compounds that demonstrated potent strand-transfer inhibitory activity were also confirmed by gel-based assay, and IC_{50} values determined from the gel-based assay were consistent with the values determined via in-house plate assay (Table 1).

Carbazole derivatives are competitive inhibitors of integrase

To investigate the strand-transfer inhibitory mechanisms and kinetics of the compounds, we determined V_{max} and K_m of the inhibition by Lineweaver–Burke plot analyses. We selected two compounds, **CA-0** and **CA-13**, for the analyses. As summarized in Table 2, larger K_m values (nM) were observed with higher inhibitory concentration, whereas V_{max} values (RU/min) did not change and remained consistent at any inhibitory concentration (Figure 3). As shown in Figure 3A and 3B, data-fitted lines of different time points converged on the Y axis, indicating that **CA-0** and **CA-13** inhibited strand-transfer in a competitive manner.

Table 1. Strand transfer and *in vitro* viral replication inhibitory activities of carbazole derivatives

	IC_{50} in strand transfer assay		Anti-HIV activity
	Plate assay (μM)	Gel assay (μM)	IC_{50} (μM)
(A) High-inhibitory group			
CA-0	5.00 ±3.31	1.24 ±0.09	0.48 ±0.06
CA-13	4.38 ±2.78	1.13 ±0.21	0.51 ±0.12
CA-1	7.94 ±4.12	2.97 ±0.21	0.92 ±0.15
CA-4	8.99 ±3.39	6.34 ±0.89	1.52 ±0.46
CA-8	6.61 ±4.17	6.38 ±0.32	0.79 ±0.07
CA-9	4.42 ±1.87	4.10 ±0.46	0.80 ±0.11
CA-12	5.93 ±3.53	3.14 ±0.04	0.69 ±0.15
(B) Intermediate-inhibitory group			
CA-2	22.50 ±2.27	ND	ND
CA-3	72.69 ±5.44	ND	ND
CA-7	11.88 ±7.66	ND	ND
CA-11	57.00 ±3.13	ND	ND
CA-14	17.37 ±1.79	ND	ND
CA-15	27.28 ±9.10	ND	ND
CA-16	20.51 ±15.11	ND	ND
CA-17	50.64 ±19.02	ND	ND
CA-18	10.68 ±8.88	ND	ND
CA-21	25.01 ±10.60	ND	ND
CA-22	16.92 ±7.32	ND	ND
CA-23	16.94 ±7.82	ND	ND
(C) Intermediate-inhibitory group			
CA-5	>100	ND	ND
CA-6	>100	ND	ND
CA-10	>100	ND	ND
CA-19	>100	ND	ND
CA-20	>100	ND	ND
(D) Previously reported inhibitor			
S-1360	4.67 ±1.89	ND	ND

Underline, indicates original compound; IC_{50}, 50% inhibition concentration; ND, not done.

Carbazole derivates have not shown intercalative activity

Due to their planar structure and their manner of competitive inhibition, we were concerned that the compounds might have the intercalative activity to destroy substrate dsDNA, rather than binding to the IN to block its enzyme activity. To clear the possibility of the intercalation, EtBr displacement assay was carried out. Since EtBr intercalates into dsDNA and makes visualization possible by growing fluorescence under UV light, intercalative activity of the test compounds can be evaluated by whether the test compounds displace incorporated EtBr out from dsDNA. As shown in Figure 4, fluorescence intensity diminished in a dose-dependent manner by actinomycin D, a compound known as a potent intercalator. In contrast, our two test compounds **CA-0** and **CA-13** did not affect fluorescence intensity, even at the highest concentration of 1 mM, suggesting that **CA-0** and **CA-13** were not intercalators.

Antiviral activity

We employed a single replication infectivity assay using HeLa4.5/EGFP cells to investigate the potency of antiviral activity. IC_{50} values of **CA-0** and the six compounds were 0.48, 0.92, 1.52, 0.79, 0.8, 0.69, 0.51 μM, respectively. The IC_{50} values of all seven compounds were 5.5 to 10.4-fold lower than that of the strand transfer assay (Table 1A). The discrepancy in IC_{50} between the two assays can be explained by stoichiometry of the inhibitor and the target enzyme in the two assays, and the estimated amount of IN in-strand transfer assay was higher than in the

Table 2. Inhibition kinetics of representative carbazole compounds **CA-0** and **CA-13**

Chemical	Concentration	V_{max} (RU/min)	K_m (nM)
CA-0	10 μM	463.16 ±63.16	30.40 ±7.80
	5 μM	402.58 ±32.21	26.21 ±7.40
	1 μM	370.14 ±84.42	12.71 ±2.02
	0 μM	454.55 ±0.02	9.18 ±1.18
CA-13	10 μM	409.70 ±35.47	19.31 ±4.68
	5 μM	439.07 ±164.74	14.83 ±0.24
	1 μM	438.08 ±53.85	11.09 ±2.42
	0 μM	429.83 ±136.46	7.08 ±0.64

Figure 3. Inhibition kinetics assays of two representative carbazole derivatives, **CA-0** and **CA-13**

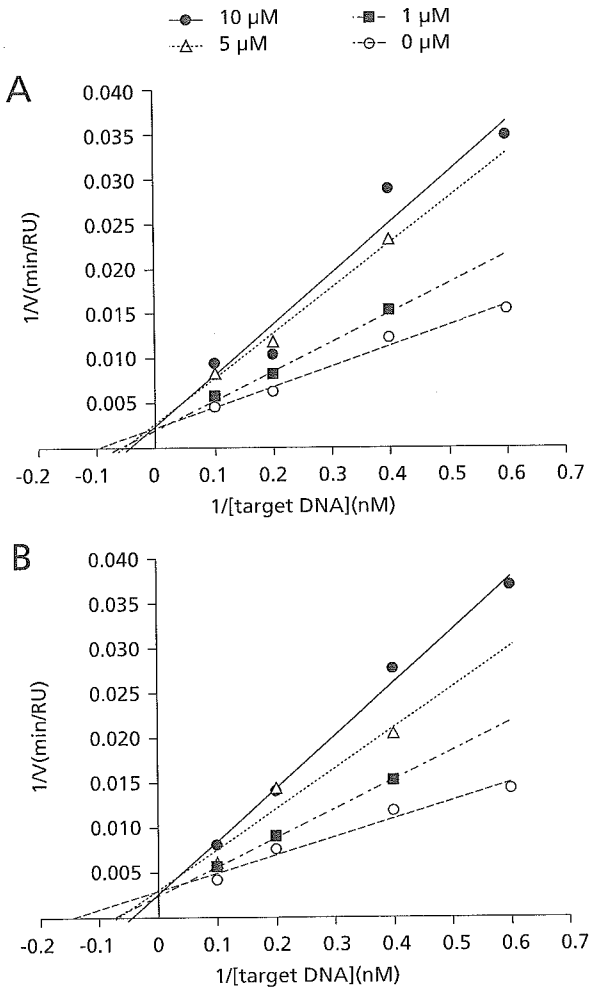

Lineweaver–Burke plot analyses of **(A) CA-0** and **(B) CA-13** are depicted.

Figure 4. Ethidium bromide displacement assays of two representative carbazole derivatives, **CA-0** and **CA-13**

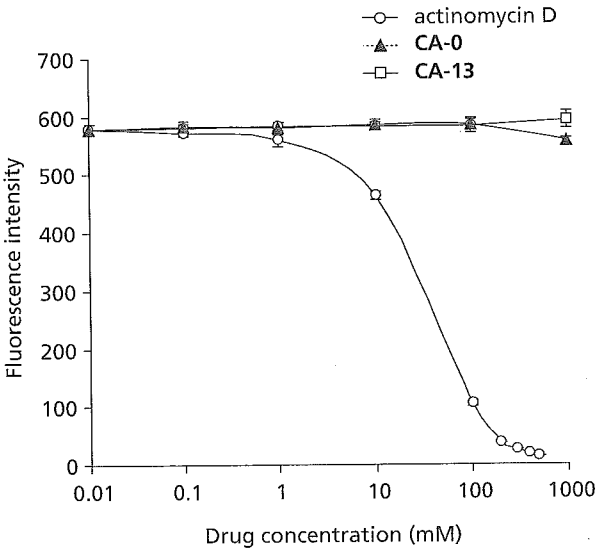

To evaluate intercalative activities of carbazole derivatives, ethidium bromide displacement assays were carried out for two representative compounds, **CA-0** and **CA-13**.

HeLa4.5/EGFP assay. Seven compounds exhibited considerable toxicity, suggesting that efforts toward decreasing toxicity are necessary for the further development of carbazole-based inhibitors.

Discussion

Carbazole, a fused phenyl-ring structure with hydrophobicity, has provided an interesting scaffold for the development of novel drugs. Staurosporine, discovered among microbial alkaloids, was the first carbazole derivative reported to demonstrate biological activity (Omura *et al.*, 1977; Furusaki *et al.*, 1978; Furusaki *et al.*, 1982), which was protein kinase C inhibition (Tamaoki *et al.*, 1986). Other carbazole derivatives have demonstrated various other activities, such as topoisomerase inhibition (Marotto *et al.*, 2002; Facompre *et al.*, 2002; Carrasco *et al.*, 2001), hypotensive activity (Furusaki *et al.*, 1982), platelet aggregation inhibition (Oka *et al.*, 1986), and anti-fungal activity (Sunthitikawinsakul *et al.*, 2003). In this report we present another possible activity of carbazole derivatives, that of HIV-1 integrase inhibitor.

As compounds with three or four fused aromatic ring structures have been reported to demonstrate intercalative activity (Fukui & Tanaka, 1996; Dziegielewski *et al.*, 2002), we initially suspected that our carbazole derivatives also have intercalative activities, penetrating and disturbing target dsDNA, resulting in pseudo strand-transfer inhibition. Indeed, several carbazole derivatives have been recognized to demonstrate intercalative activity (Facompre *et al.*, 2002; Long *et al.*, 2002). We confirmed that actinomycin D, which is a well-known intercalator (Ross *et al.*, 1979; Wilson & Jones, 1982), demonstrated strand-transfer inhibition in our assay (data not shown). However, taking into consideration the data that our carbazole derivatives inhibited strand-transfer in a competitive manner, and also that the compounds could not displace EtBr out from dsDNA, we assume that our derivatives bind to part of the IN molecule, to the region responsible for DNA target

binding or to the catalytic site responsible for strand-transfer activity.

To understand in greater detail the substituents responsible for strand-transfer inhibitory activity, we analysed 23 carbazole derivatives, and classified them into three categories according to their levels of inhibition (Table 1). Six compounds were classified as the high-inhibition group, which demonstrated IC_{50} of less than 10 μM, 12 compounds were classified as the intermediate group, which demonstrated IC_{50} of greater than 10 μM and less than 100 μM, and five compounds were classified as the non-inhibition group, in which we did not observe significant inhibition even at the highest concentration tested (100 μM).

Comparing the compounds between and within these three categories, we recognized three factors responsible for strand-transfer inhibition. The first and most important factor is the incidence of a 2-dimethylaminoethyl group at position R2 (Figure 1A).

CA-8, which possesses a 2-dimethylaminoethyl group at position R2, demonstrated high inhibitory activity (IC_{50}: 6.61 ±4.17 μM), but **CA-19** (IC_{50}: >100 μM), which possesses a phenyl ring structure at the same R2 position, did not demonstrate inhibitory activity. Thus, it is clear that the incidence of a 2-dimethylaminoethyl group, which has a basic property, is critical for strand-transfer inhibition activity. Indeed, we recognized that all compounds in the "high-inhibitory group" and "intermediate-inhibitory group" had this basic substituent at position R2 (Table 1A, 1B, Figure 2). In contrast, three of five compounds in the "non-inhibitory group" had the phenyl ring structure at R2 position. It is thought that these compounds might bind to the acidic region on the IN molecule and compete with the target dsDNA.

The second factor is the incidence of a methyl (Me) group at position R5, R6 or R7. We recognized that compounds in the high inhibitory group had at least one Me group at the R5, R6 or R7 position (Table 1A, Figure 2). Comparing **CA-1** (IC_{50}: 7.94 ±4.12 μM), **CA-4** (IC_{50}: 8.99 ±3.39 μM), and **CA-12** (IC_{50}: 5.93 ±3.53 μM) with **CA-15** (IC_{50}: 27.28 ±9.10 μM), it is clear that the incidence of an Me group within the R5 to R7 positions was an important factor for enhanced inhibitory activity. It seems that the position of the substituent may not be critical between R5 and R6, as we did not see significant differences between **CA-1** (IC_{50}: 7.94 ±4.12 μM) and **CA-12** (IC_{50}: 5.93 ±3.53 μM), and also between **CA-8** (IC_{50}: 6.61 ±4.17 μM) and **CA-9** (IC_{50}: 4.42 ±1.87 μM).

According to the IC_{50} levels of **CA-5** (>100 μM), **CA-6** (>100 μM) and **CA-11** (>100 μM), it appears that bulky substituents at the R5 position have a negative effect on inhibition (Table 1C, Figure 2). Furthermore, the inhibition potential of the three compounds **CA-1** (IC_{50}: 7.94 ±4.12 μM), **CA-16** (IC_{50}: 20.51 ±15.11 μM) and **CA-17** (IC_{50}: 50.64 ±19.02 μM) depended on the molecular size of their R5 substituents. It is probable that the R5 substituents of these compounds were too large and that they interfered with surrounding molecules forming the binding site (Table 1A, 1B, Figure 2). These data indicate that the binding site of carbazole might have a space limitation, and thus the size and shape of the molecules may be important factors for inhibitor activity.

The third factor is the substituent at position R9. Comparing **CA-20** (IC_{50}: >100 μM), **CA-21** (IC_{50}: 25.01 ±10.60 μM) and **CA-22** (IC_{50}: 16.92 ±7.32 μM), these three compounds were identical, with the exception of the substituent at position R9 (Table 1B, 1C, Figure 2). **CA-21** and **CA-22** have hydroxyl residue and a methoxy group at position R9, respectively. We noticed a significant difference in inhibitory activity between **CA-20** and **CA-21**, and between **CA-20** and **CA-22**, suggesting the possibility that both the hydroxyl group and the methoxy group at R9 formed hydrogen bonds with the amino acid molecules forming the binding sites, as these two substituents have the potential to be hydrogen bond acceptors. It appears that hydroxyl and methoxy groups have similar effects on strand-transfer inhibitory activities. In addition to the above three factors, we found that molecular interaction between R8 and R9 substituents, and their arrangement, are also important determinants for efficient inhibitory activity. **CA-3**, with two methoxy groups at R8 and R9, appears to have a bulky arrangement of the two side chains, and demonstrated an IC_{50} of 72.69 ±5.44 μM, whereas **CA-14** and **CA-18**, which were expected to have horizontal arrangements, demonstrated lower IC_{50} values of 17.37 ±1.79 μM and 10.68 ±8.88 μM, respectively (Table 1B, Figure 2).

To summarize these structural elements, and to understand the common structure of molecules that demonstrated strand-transfer inhibitory activity, we superposed inhibitor structures having significant strand-transfer inhibition (**CA-0**, **CA-1**, **CA-4**, **CA-8**, **CA-9**, **CA-12** and **CA-13**) (Figure 5A), and the structures of compounds with no inhibition (**CA-5**, **CA-6**, **CA-10**, **CA-19** and **CA-20**) (Figure 5B). In comparing these two overlapped figures, we found that the compounds with inhibitory activity share a largely identical structure and similar molecular size. In contrast, the non-inhibitory compounds had larger and more uneven-shaped side chains. Overall, the superposed structures indicate that the molecules should be planar and have basic diethylaminoethyl groups to demonstrate strand-transfer inhibitory activity.

In conclusion, we have identified a small molecular weight compound with a carbazole scaffold, which can be the lead compound for developing novel IN inhibitors. Furthermore, analysing the IN inhibitory mechanisms of

Figure 5. A structural comparison between high/intermediate inhibitory compounds and non-inhibitory compounds

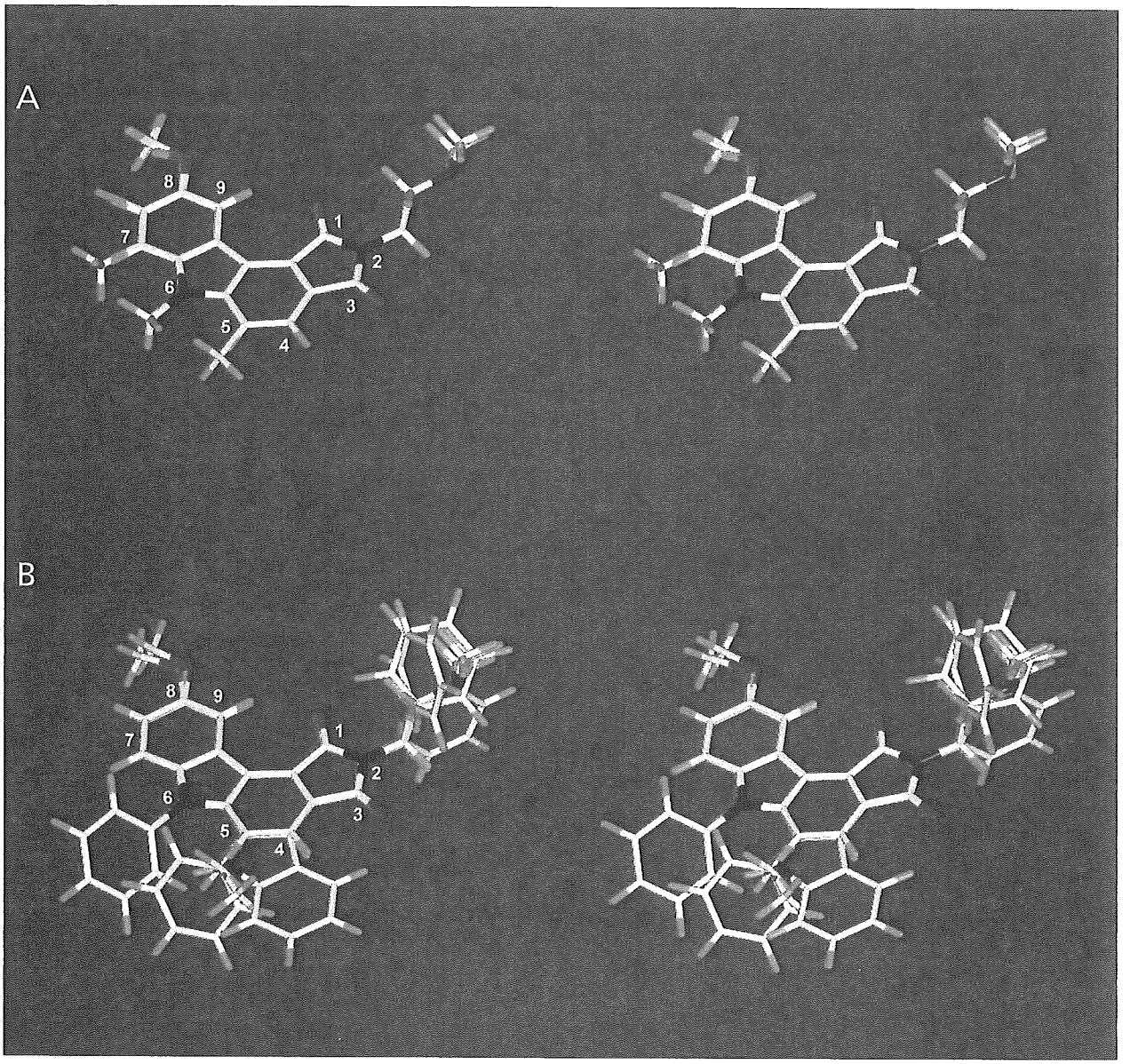

Superposed structures of **(A)** five non-inhibitory compounds, **CA-5**, **6**, **10**, **19** and **20**, and **(B)** seven inhibitory compounds, **CA-0**, **1**, **4**, **8**, **9**, **12** and **13**, are demonstrated in stereo-view images. In both figures, residue numbers are indicated beside the structures. Red, dark blue and light blue indicate oxygen, nitrogen and hydrogen molecules, respectively. Green indicates chlorine or fluorine molecules. SYBYL software Version 6.9.1 running on an SGI Fuel workstation was used to construct the figures.

carbazole derivatives may yield more detailed information regarding HIV-1 IN structure and function.

Acknowledgements

This study was supported by a grant from the Human Sciences Foundation, the Organization of Pharmaceutical Safety and Research of Japan and the Ministry of Health, Labor and Welfare of Japanese Government. This study was partly supported by the Program for Promotion of Fundamental Studies in Health Sciences of the National Institute of Biomedical Innovation (NIBIO)

We would like to thank Dr. Haruo Tanaka and Takuro Shiomi, professor and associate professor of Kitazato